Adsorption of nucleotides on biomimetic apatite: The case of adenosine 5′ monophosphate (AMP)

K. Hammami[a,b], H. El Feki[a], O. Marsan[b], C. Drouet[b,*]

[a] *Laboratoire de L'Environnement et de Sciences de Matériaux (MESLAB), Faculté des sciences de Sfax, BP 802 3018 Sfax, Tunisia*
[b] *CIRIMAT Carnot Institute – "Phosphates, Pharmacotechnics, Biomaterials" group, University of Toulouse, CNRS/INPT/UPS, ENSIACET, 4 allée Emile Monso, 31030 Toulouse Cedex 4, France*

Keywords:
Nanocrystalline apatite
Adenosine monophosphate
Adsorption
Nucleotide
Diagenesis
Vibrational spectroscopy

A B S T R A C T

This work investigates the interaction between the nucleotide adenosine 5′ monophosphate molecule (AMP) and a biomimetic nanocrystalline carbonated apatite as a model for bone mineral. The analogy of the apatite phase used in this work with biological apatite was first pointed out by complementary techniques. AMP adsorption isotherms were then investigated. Obtained data were fitted to a Sips isotherm with an exponent greater than one suggesting positive cooperativity among adsorbed molecules. The data were compared to a previous study relative to the adsorption of another nucleotide, cytidine monophosphate (CMP) onto a similar substrate, evidencing some effect of the chemical nature of the nucleic base. An enhanced adsorption was observed under acidic (pH 6) conditions as opposed to pH 7.4, which parallels the case of DNA adsorption on biomimetic apatite. An estimated standard Gibbs free energy associated to the adsorption process ($\Delta G^{\circ}_{ads} \cong -22$ kJ/mol) intermediate between "physisorption" and "chemisorption" was found. The analysis of the solids after adsorption pointed to the preservation of the main characteristics of the apatite substrate but shifts or enhancements of Raman bands attributed to AMP showed the existence of chemical interactions involving both the phosphate and adenine parts of AMP. This contribution adds to the works conducted in view of better understanding the interaction of DNA/RNA and their constitutive nucleotides and the surface of biomimetic apatites. It could prove helpful in disciplines such as bone diagenesis (DNA/apatite interface in aged bones) or nanomedicine (setup of DNA- or RNA-loaded apatite systems). Also, the adsorption of nucleic acids on minerals like apatites could have played a role in the preservation of such biomolecules in the varying conditions known to exist at the origin of life on Earth, underlining the importance of dedicated adsorption studies.

1. Introduction

Apatites are a large group of minerals, generally crystallizing in the hexagonal structure (space group $P6_3/m$), and whose main representatives are hydroxyapatite or else fluorapatite. In particular, hydroxyapatite ($Ca_{10}(PO_4)_6(OH)_2$, HA) is the basic mineral constituent of enamel microcrystals; in contrast, the mineral part of bone (65–75 wt.%, depending on age and sex) and of dentin is composed of a hydrated nonstoichiometric apatite phase formed of nanosized crystals and exhibiting a low degree of crystallinity [1,2]. Besides biological apatites, various studies have been devoted to the preparation, under close-to-physiological conditions (temperature, pH), of synthetic nanocrystalline apatites analogous to bone mineral [3–5]. As in bone, "biomimetic" apatite nanocrystals have the particularity to expose a structured but metastable hydrated surface layer, containing labile ions (e.g. Ca^{2+}, HPO_4^{2-}, CO_3^{2-}...) located in "non-apatitic" environments, as evidenced previously [6–13]. These surface ions were also shown to be easily "exchangeable" in solution with ions from the surrounding medium [11,14,15], leading to very peculiar surface properties [16]. Also, surface ions play a primordial role in adsorption mechanisms [17,18]. In the field of bone repair materials, these characteristics are important for the interactions between apatite-based implants and the biological environment of implantation. In *postmortem* conditions, bone diagenesis and bone/DNA interactions are also thought to be modulated/controlled by surface properties of apatite nanocrystals [19,20].

* Corresponding author at: CIRIMAT, Ensiacet, 4 allée Emile Monso, 31030 Toulouse Cedex 4, France. Tel.: +33 05 34 32 34 11.
E-mail address: Christophe.Drouet@ensiacet.fr (C. Drouet).

Considering adsorption on apatite nanocrystals, substantial variations of adsorption parameters can be observed depending on the maturation state of the apatite [18]. Generally speaking, the adsorption affinity constant tends to increase when the initial maturation time of the apatite substrate increases, while the maximum amount adsorbed decreases. The mineral apatitic matrix plays a crucial role in calcified tissues and biomaterials, and many macromolecules have been classified as initiator or inhibitor of crystal growth although for a given substance the role is not so clear and could depend, for example, on the local concentration or on the state of solute or solid fractions of this given substance [21]. In the biomaterials field, it has been suggested that molecules interacting with calcium phosphates may play a crucial role in the recruitment of cells and their expression and that they are strongly involved in the biointegration of implants [22,23]. The utilization of nanocrystalline apatite materials as bone grafts may reduce the need for autologous bone graft, increase the stability of the implant, lead to faster bone regeneration, and facilitate the healing process [24]. In the biomineralization context, the ability of apatite to adsorb various types of molecules (proteins, other biomolecules, and various drugs) can play a determining role in calcified tissues. These phenomena are considered to control in particular apatite nucleation, growth and dissolution in vivo [25,26].

The exploration of adsorption processes is interesting in itself, as it may provide a background for both the fundamental understanding (bio)molecule/apatite interactions and for the development of drug delivery systems based on apatite materials. In the present contribution, we inspected the interaction existing between a model nucleotide, adenosine 5′ monophosphate (AMP), and a biomimetic apatite compound. AMP is a nucleotide encountered, as a monomer "building block", in macromolecules of DNA and RNA. Being able to appreciate the type of interaction existing between AMP and apatite surfaces may help understanding the adsorption of the larger DNA or RNA molecules. Apatites and other calcium phosphates nanoparticles have for example been investigated as drug carriers to deliver genetic materials to eukaryotic cells [27,28]. The interaction between AMP and precipitated calcium phosphate was reported in the 1990s [29] but on substrates with undetermined physicochemical features.

AMP is an ester of phosphoric acid and the nucleoside adenosine. It is also the mono-phosphate version of adenosine triphosphate known to control energy storage processes in live cells. From a biochemical viewpoint, 5′-adenosine monophosphate-activated protein kinase (AMPK) is an enzyme that plays a role in cellular energy homeostasis. In the presence of AMP, the activity of AMPK is increased so that AMPK is regulated by AMP [30]. The effects of AMP are two-fold: a direct allosteric activation, and making AMPK a poorer substrate for dephosphorylation. Because AMP affects both the rate of AMPK in the phosphorylation positive direction and dephosphorylation in the negative direction, the cascade is ultra-sensitive [30]. Nucleotides such as AMP, but also the di-phosphate ADP and tri-phosphate ATP versions, are therefore recognized as important biomolecules in metabolic interconversions. Nucleotide derivatives such as ATP (adenosine triphosphate) can also be present in the extracellular fluid under physiologic circumstances [31]. From a more applied viewpoint, the presence of AMP and its interaction with AMPK biochemistry has also tentatively been associated to the control of vascular calcifications [32].

The aim of this work was to study the physicochemical interaction existing in solution between the AMP nucleotide and a well-characterized synthetic biomimetic apatite. The interaction phenomena were determined via adsorption reactions involving physicochemical characterization of the liquid and solid phases, including with vibrational spectroscopy techniques (FTIR and RAMAN).

2. Materials and methods

2.1. Synthesis of biomimetic apatite

The synthesis of biomimetic apatite and the analysis of physicochemical features showing their biomimetism to bone mineral was reported previously [19]. In the present work, a biomimetic carbonated apatite sample analogous to bone mineral was prepared similarly as before, by a double decomposition reaction, at physiological pH and room temperature (22 °C), by mixing a calcium nitrate $Ca(NO_3)_2{\cdot}4H_2O$ solution (52.2 g in 750 ml of deionized water) and a solution containing both phosphate solution of ammonium hydrogenphosphate $(NH_4)_2HPO_4$ and sodium bicarbonate $NaHCO_3$ (90 g of each in 1500 ml of deionized water). The calcium solution was poured rapidly into the phosphate and carbonate solution. The excess of phosphate and carbonate ions used in these conditions had a buffering effect and allowed the pH to stabilize around 7.4. The suspension was left to mature at room temperature for 7 days and was then filtered on a Buchner funnel, thoroughly washed with deionized water, freeze-dried and stored in a freezer (−18 °C) to avoid further alteration of the apatite nanocrystals. The apatite powder, referred to as "hac-7d", was then sieved and the size fraction 100–200 μm was used for all experiments.

2.2. Adsorption of adenosine 5′ monophosphate (AMP) onto biomimetic apatite

Adenosine 5′ monophosphate (AMP) was used as adsorbate in this study, in the form of its dissolved hydrated disodium salt, $Na_2AMP{\cdot}xH_2O$ (purity > 99.0, HPLC grade, Sigma–Aldrich) of formula $C_{10}H_{12}N_5Na_2O_7P$. Fig. 1a reports the corresponding developed chemical formula of the anhydrous salt.

The AMP adsorption isotherm (at 22 °C) was constructed by drawing the adsorbed amount N_{ads} versus the equilibrium concentration C_{eq} in solution, varying from 0 to 2 mmol/l. For each datapoint, 60 min of contact was selected as this time was preliminarily shown to allow equilibration of the system. All experiments were run at least in duplicate, and involved the immersion of 20 mg of nanocrystalline apatite powder hac-7d in an AMP solution (5 ml) of increasing concentrations and in KCl 10^{-2} M buffer solution, at room temperature and at pH 7.4. In each case, the samples were centrifuged at 5000 rpm for 10 min and filtered onto Millipore (0.2 μm). The clear solution was removed via pipetting for analysis. The amount of adsorbed AMP was determined by comparison between the initial amount of AMP dissolved in the adsorption medium and the residual amount present after the selected contact time. Spectrophotometry analyses (Shimadzu UV 1800) were run in the UV domain, by following the optical density (absorption) at 259.4 nm (see Fig. 1b). A calibration curve (correlation factor of 0.9998) was previously drawn for standard solutions of AMP concentrations ranging from 0.0078 to 0.078 mg/ml. All standard solutions were prepared with deionized water.

2.3. Physicochemical characterization

The solid phases were subjected to XRD, FTIR/RAMAN, TG-TDA analyses, as well as chemical titrations for Ca and inorganic phosphate and scanning electron microscopy (SEM/EDX) observations. The details are as follows.

X-ray diffraction (XRD) analysis was performed by means of a CPS 120 INEL powder diffractometer equipped with a graphite monochromator and using the $CoK_{\alpha 1}$ radiation (λ = 1.78892 Å). The samples were scanned in the 2θ range from 20° to 80° with a step size of 0.02° and a counting time of 1 s per step. Mean crystallite

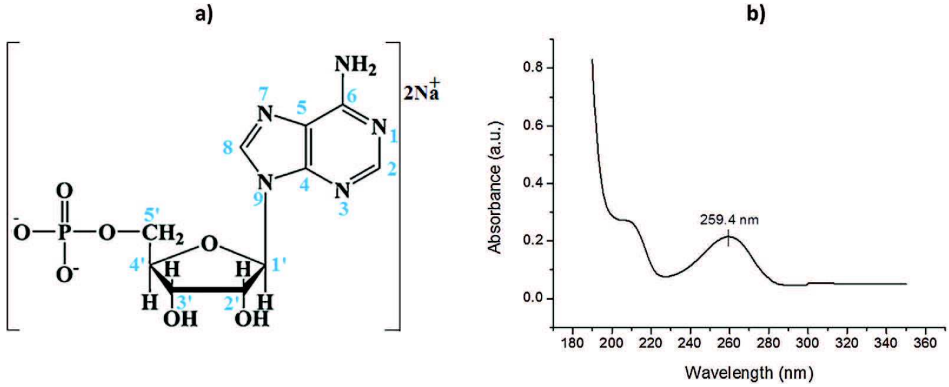

Fig. 1. (a) Molecular structure of adenosine 5′-monophosphate (AMP) disodium salt, and (b) UV absorption maximum used for titration in solution.

lengths along the *c*-axis were then estimated from the (0 0 2) line broadening using Scherrer equation.

An FTIR (Thermo Nicolet 5700) spectrometer was used to study the vibrational features of the compounds. 2 mg of dried sample powder was compacted with 300 mg potassium bromide using a hydraulic pressure. For each spectrum, 64 scans between 400 and 4000 cm^{-1} were recorded, with a resolution of 4 cm^{-1}.

Raman analyses of the samples, in the range 400–1500 cm^{-1}, were generated on a confocal Labram HR800 micro-spectrometer. The samples were exposed in backscattering mode to an AR-diode laser (λ = 532 nm) with a power of 17 mW. Measurements were carried out with a spectral resolution of 3 cm^{-1}. The uncertainty on Raman shifts (<1 cm^{-1}) have been calibrated using a silicon standard at 520.7 cm^{-1}. An optical objective ×100 was used for all analyses, conferring to the system a lateral resolution of 0.7 μm and an axial resolution of 2.7 μm. The spectra reported in this work are the average of 3 spectral accumulations, each being exposed for 120 s.

The chemical composition of the apatite compound synthesized here was determined from titrations by complexometry for the determination of the calcium content, by spectrophotometry for the total phosphate content (determination of the sum of PO_4^{3-} and HPO_4^{2-} ions, using the phospho-vanado-molybdenic method [33] and by coulometric method (UIC, Inc. CM 5014 coulometer with CM 5130 acidification unit) for the carbonate content.

Thermogravimetric analyses (TG-DTA) were performed for evaluating the amount of hydration water contained in the AMP sodium salt, using a Setaram Instrumentation SETSYS evolution system, with a heating rate of 5 °C/min, from 25 °C to 900 °C in air.

The specific surface area, S_{BET}, was determined using the BET method using nitrogen adsorption, on a Tristar II Micromeritics apparatus.

Zeta potential (electrophoretic mobility) was determined at 25 °C using a Malvern Zetasizer Nano Analyzer apparatus, with disposable zeta cells, after dispersion of the powder preliminarily stabilized at different pH values (in the range 6–9.5) and syringe-filtered for avoiding the sedimentation of large aggregates (>1 μm) during the analyses.

Morphology and particle dimensions/agglomeration state of pure hac-7days and after adsorption of different amounts of AMP were followed using a scanning electron microscope (SEM) LEO 435 VP at a voltage of 15 kV, equipped with an EDX elemental analyzer. Transmission Electron Microscope (TEM) was also performed to observe the constitutive nanocrystals of carbonated nanocrystalline apatite, using a JEOL JEM1400 microscope under 120 kV (current of 76 μA). For allowing TEM observations, the apatite sample was suspended in ethanol under ultrasonic treatment prior to direct deposition on a copper grid and air-drying.

3. Results and discussion

The hac-7d apatite substrate used in this study was first characterized by various complementary techniques as was previously done [19]. X-ray diffraction (XRD) analysis indicated (Fig. 2a) that the sample was single-phased and composed of a biomimetic nanocrystalline apatite, and the application of Scherrer's formula [34] led to the mean crystallite dimensions of ca. 19 nm (length) and ca. 5 nm (width). Thus, analyses revealed physicochemical features very close to those of bone mineral [1,35], with the following other main features: Ca/(P + C) ≅ 1.36 and $\%CO_3$ ≅ 3.6 wt.%. SEM observations (Fig. 2b) showed the aggregated shape of the constitutive particles, and the specific surface area measurement by the BET method led to S_{BET} = 180 m^2/g. Fig. 2c shows the typical plate-like morphology of constitutive crystals for such carbonated apatite, evidencing their nanosize.

The evolution of the amount N_{ads} of AMP adsorbed in KCl 10^{-2} M and at T ≅ 20 °C and pH 7.4 was recorded as a function of the equilibrium concentration C_{eq} in the solution. The exact amount of AMP was corrected by the hydration water contained in the starting sodium salt $Na_2AMP{\cdot}xH_2O$, where "x" was determined by TG analysis as being equal to 4.6. The resulting adsorption isotherm is plotted in Fig. 3.

Sorption isotherms are usually fitted, by default, using a simple Langmuir equation or the Freundlich or Temkin derived models. However, surface heterogeneities or specific adsorbate/adsorbent interactions may lead to significant deviation from these models, as was pointed out recently in the case of tetracycline adsorption for example [36]. The more general Sips model (or Langmuir–Freundlich) may often allow obtaining a better assessment of adsorptive behaviors, due to its broader character. This model can be described by the equation:

$$N_{ads} = N_m \cdot \frac{K_S \cdot C_{eq}^m}{1 + K_S \cdot C_{eq}^m} \quad \text{Sips isotherm}$$

where N_{ads} is the amount of AMP adsorbed, N_m is the maximal monolayer coverage and where K_S and "m" are respectively the Sips constant and exponent parameter. When applied to our experimental dataset, a correlation coefficient of R^2 = 0.9794 was obtained suggesting a relatively good agreement with the Sips model, with the parameters: N_m = 0.019 ± 0.006 mmol/g, K_S = 1.14 ± 0.98 and m = 1.25 ± 0.45. Despite non-negligible uncertainties, it is interesting to inspect further these values. For example, the maximum adsorbed amount N_m reaches 0.019 mmol/g (19 μmol/g), which is about 4 times lower than the value found for the adsorption of another nucleotide, cytidine monophosphate CMP (80.8 μmol/g) on a similar type of substrate. Since the chemistry of the two

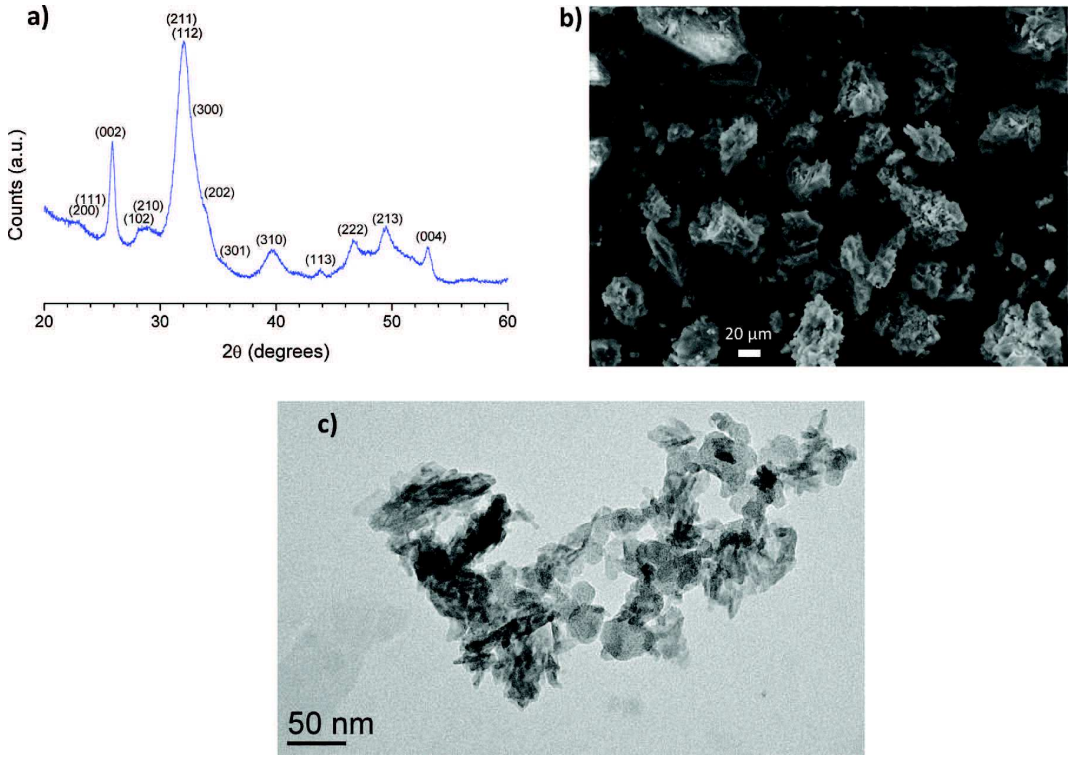

Fig. 2. (a) XRD pattern (with indexation relative to the hydroxyapatite JCPDS card 09-432), (b) SEM observation of the apatite substrate hac-7d prepared in this work, and (c) typical morphology of constitutive nanocrystals (TEM).

nucleotides differs only by the nature of their nucleic bases (adenine being a puric base with two organic cycles, and cytosine being a pyrimidic base with a single cycle), the greater adsorption amount found with CMP can presumably be linked to a greater affinity of the surface for cytosine rather than adenine. It is however at this stage not possible to suggest molecular orientations for AMP or CMP adsorbed on apatite: additional considerations, possibly through molecular dynamics, would be needed. Zeta potential measurements however indicated a somewhat less negative value (-20 ± 2 mV instead of -30.9 ± 1.8 mV at pH 6; and -23.9 ± 1.3 mV instead of -28.6 ± 2.2 mV at pH 9.5) in the presence of adsorbed AMP which agrees well with an increased exposure of the nucleic base on the particle surface, due to adsorption. The order of magnitude of the zeta potential found here for the apatitic substrate is, as can be expected, close to other measures done on similar systems (e.g. [37]); and in the present study, the zeta potential remained negative in the pH range 6–9.5 even in the presence of adsorbed AMP throughout the adsorption isotherm. This can be linked to the limited amount of adsorbed AMP molecules on the apatitic surface.

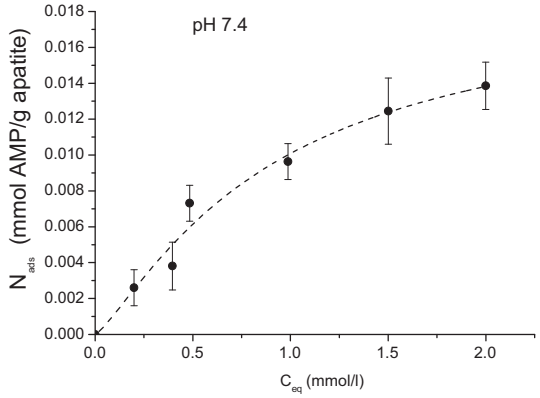

Fig. 3. Adsorption isotherm of AMP onto nanocrystalline apatite hac-7d, at pH 7.4, 20 °C and in KCl 10^{-2} M.

Of particular interest also is the value of "m", as it is thought to convey information on the heterogeneous character of the surface and on the positive or negative cooperativity between adsorbed molecules, as was recently reminded [36]. A value of "m" greater than one is generally considered to suggest a situation of "positive" cooperativity between adsorbed molecules, whereas the contrary is considered for m lower than unity. Recently Choimet et al. (publication in progress) reported a similar study has been run on the adsorption on biomimetic apatite of another nucleotide, cytidine 5′ monophosphate (CMP). In that case, similarly to the present study ($m = 1.25$), a value of m greater than one ($m = 1.20$) was obtained for Sips modeling of the adsorption isotherm. Consequently, both AMP and CMP adsorption on biomimetic apatite seem to be accompanied by a favorable positive cooperativity between adsorbed molecules.

The value of the constant K_S also conveys some physical meaning, related to the Gibbs free energy of the adsorption process, as was recently reminded and exploited in the case of tetracycline adsorption on biomimetic apatite [36]. The following equation allows one to evaluate ΔG°_{ads} from the value of K_S (re-repressed for C_{eq} in mol/l):

$$K_S = \exp\left(-\frac{\Delta G^{\circ}_{ads}}{RT}\right)$$

This leads to the negative value $\Delta G^{\circ}_{ads} \cong -22$ kJ/mol (uncertainty estimated to ± 1 kJ/mol), indicating a favorable adsorption

of AMP on biomimetic apatite in standard conditions. This value is similar to those found recently for the adsorption of CMP (−19 kJ/mol) and for tetracycline (−22 kJ/mol) on nanocrystalline apatite: this order of magnitude is consistent with the typical strength of an electrostatically mediated surface–molecule interaction and is found to fall in an intermediate situation between what is generally considered as physisorption and chemisorption.

A previous study on the adsorption of DNA on biomimetic apatite has pointed out the effect of pH on the adsorbed amount [19]. In particular, an increased adsorption was found when the contact between the substrate and the biomolecules was undergone in acidic conditions. In order to inspect this at a single nucleotide level (as a "building block" of DNA), we investigated here the adsorption of AMP at pH 6. The adsorption isotherm obtained in this acidic condition is plotted in Fig. 4. As evidenced on this figure, for a given equilibrium concentration, the adsorption amount was found to increase significantly upon pH drop from 7.4 to 6. Again, the data were satisfyingly fitted to the Sips adsorption model ($R^2 = 0.9988$), with however modified

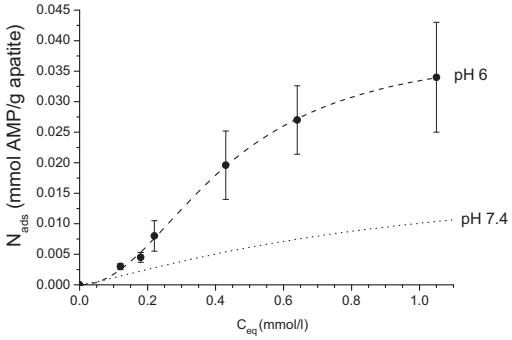

Fig. 4. Adsorption isotherm of AMP onto nanocrystalline apatite hac-7d, at pH 6, 20 °C and in KCl 10^{-2} M (compared to data obtained previously at pH 7.4).

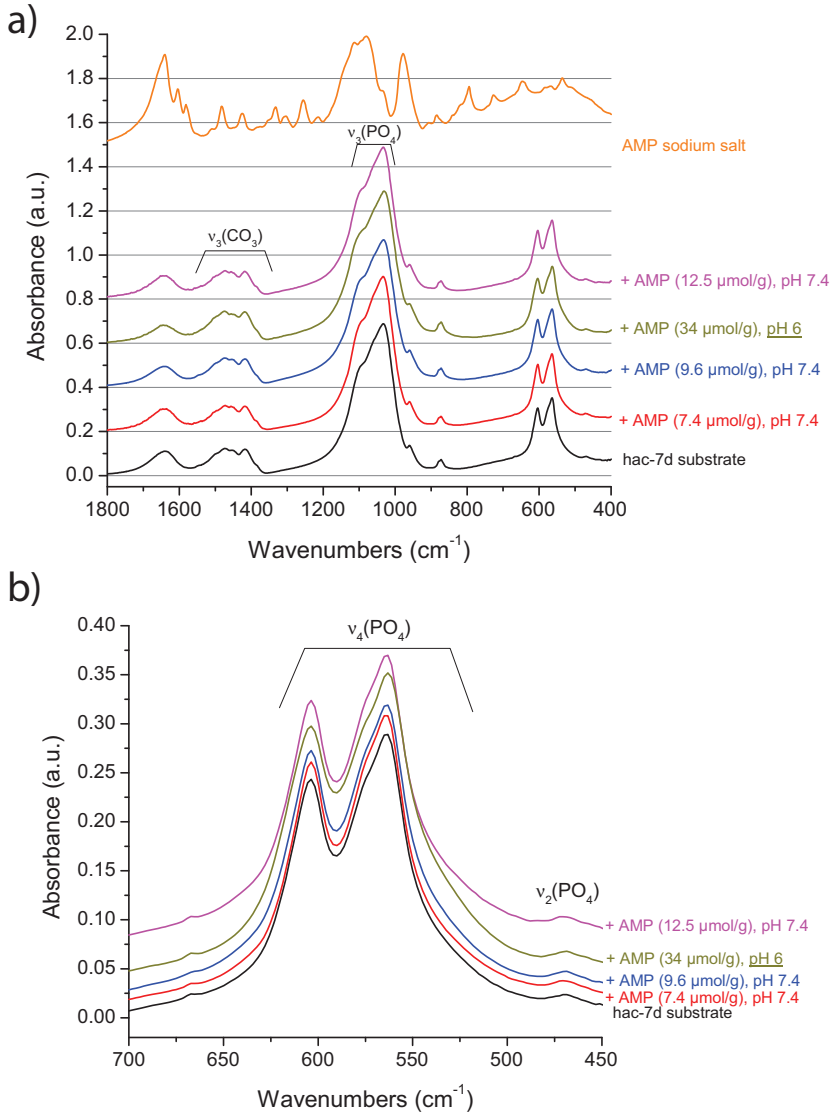

Fig. 5. (a) FTIR analysis of the apatitic substrate before and after AMP adsorption for varying coverages, and spectrum of AMP sodium salt. (b) zoom on the $\nu_2\,\nu_4(PO_4)$ domain.

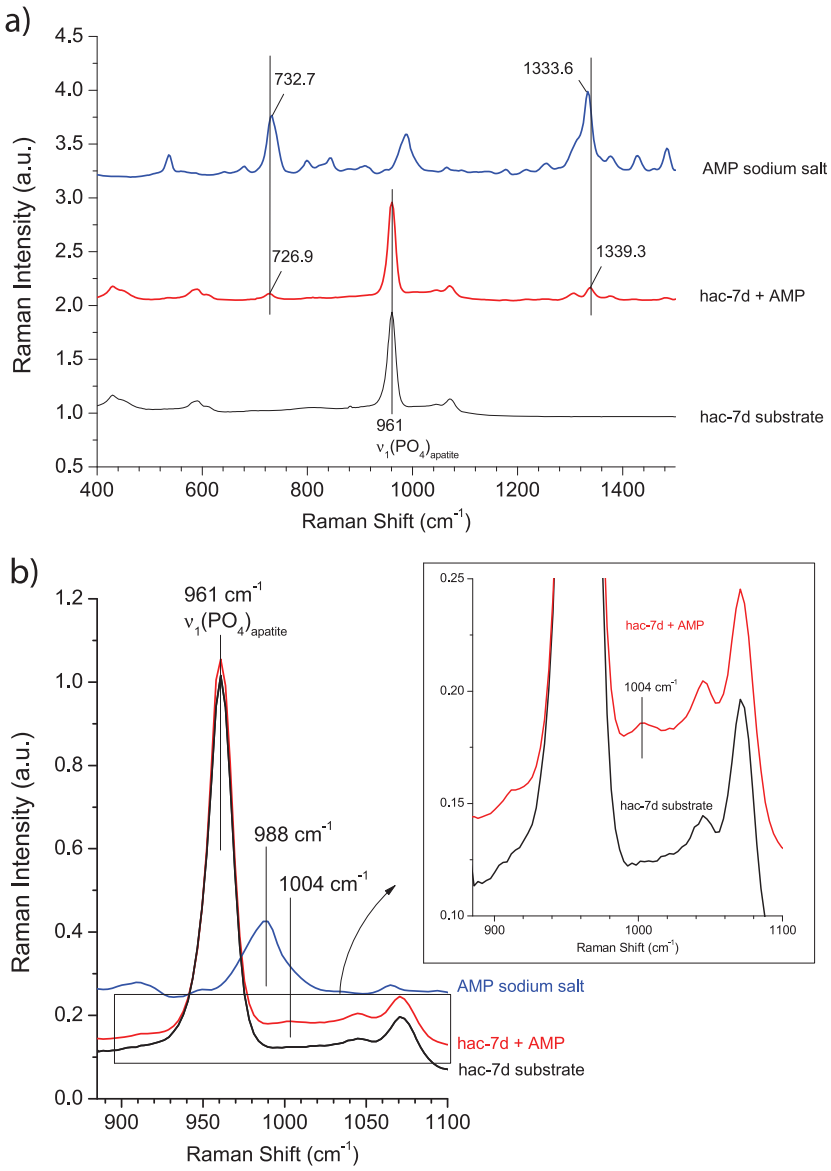

Fig. 6. Raman micro-spectroscopy analysis of the hac-7d substrate before or after adsorption (pH 7.4) and of AMP sodium salt: (a) general spectrum in the range 400–1500 cm^{-1} and (b) zoom around the $\nu_1(PO_4)_{apatite}$ vibration domain.

parameters as follows: $N_m = 0.039 \pm 0.002$ mmol/g, $K_S = 5.71 \pm 1.12$ and $m = 2.09 \pm 0.12$. While remaining in the stability domain of apatite, these findings point to a situation where the affinity of the surface for the AMP molecules becomes enhanced in acidic medium, which is evidenced by the significant increase of the constant K_S; also the maximum amount reaches 0.039 mmol/g which is about twice the value found for pH 7.4. The value of "m" close to 2 also depicts a situation with significant cooperativity between adsorbed species, in an even greater scale than at neutral pH.

This effect of pH on the adsorption of nucleotides on biomimetic apatites is, to our knowledge, the first of the kind. It parallels what was previously noticed for the adsorption of DNA [19], thus suggesting that this effect is not a peculiarity of this macromolecule but that it can probably be ascribed to surface modifications of biomimetic apatites upon acidification. It may be assumed quite reasonably that the protonation of surface phosphate ions is bound to increase noticeably upon acidification of the medium in which it is emerged. This increased protonation may be at the origin of this adsorption enhancement effect, either 1) by moving the surface charge toward more positive values more prone to attract the phosphate end-groups of AMP molecules, or 2) by promoting the release in the solution of protonated phosphate ions (less attracted by calcium due to a diminished charge) and their simultaneous replacement by AMP molecules. Further studies are undergoing on the adsorption of various (bio)molecules onto biomimetic apatite under varying pH values, which should enables us in the future to explain the present observation with more details.

The solids were analyzed after adsorption by vibrational spectroscopy techniques. FTIR analyses (Fig. 5a) showed that the apatite substrate did not undergo noticeable changes upon adsorption, as in all cases the bands characteristic of a carbonated apatite phase were noticed [13,38–42]. In particular, the level of carbonation

was found to remain unchanged, as could be assessed by the relative intensity of the $\nu_3(CO_3)$ band when compared to $\nu_3(PO_4)$ [43]. This was observed independently of the pH value of 7.4 or 6. The chemical environments in the apatite substrate, as followed on the $\nu_2\nu_4(PO_4)$ domain, also remained essentially unchanged by FTIR upon adsorption (Fig. 5b), although the global (averaging) character of these transmission analysis do not lead to specific surface features. The characteristic bands of AMP could not be visualized on these spectra, which can be attributed to the small amount of adsorbed molecules on the surface of the nanocrystals, and to the above mentioned lack of surface-specific analysis by this technique. Moreover, phosphate and carbonate groups from apatite as well as water environments provide many rather intense absorption bands in infrared spectroscopy, which does not facilitate the detection of AMP features.

A complementary analysis was thus carried out by Raman micro-spectroscopy. The bands relative to (adsorbed) AMP become detectable besides those of the apatitic substrate, as can be typically seen in Fig. 6. Interestingly, some of the AMP characteristic bands appear shifted as compared to those of pure AMP (Fig. 6a).

This is in particular the case for the relatively intense bands linked to the skeleton vibrations of the adenine ring [44] at 726.9 instead of 732.7 cm^{-1} (assignable to adenine ring breathing mode [45]) and at 1339.3 instead of 1333.6 cm^{-1} (in-plane adenine ring mode [45]). They point to a situation where the adenine part of the molecule gets modified by the sorption process. Such a shift in Raman band position can be attributed to surface chemical interactions existing between neighboring AMP molecules (as suggested by the positive cooperativity of the Sips model) and/or between AMP and the surface of apatite nanocrystals.

On the other hand, the phosphate group of AMP is responsible for the presence of a rather intense band located, for the AMP sodium salt, around 988 cm^{-1}. This band is attributable to the vibration mode $\nu_1(PO_4)_{AMP}$ [46] where the phosphate group is in non-protonated form [47]. Interestingly, the Raman spectral region around this position (Fig. 6b) appears significantly modified in the case of AMP adsorbed on apatite, with a clear band rise at ca. 1004 cm^{-1} and no detection of the 988 cm^{-1} band. A low intensity Raman contribution at 1005 cm^{-1}, also attributed to the (non-protonated) phosphate group of AMP, has already been reported for pure AMP [47]; and a close analysis of Raman data for the AMP sodium salt used in the present work allows one to detect at 1004 cm^{-1} a shoulder to the main 988 cm^{-1} band (Fig. 6b). However, in the case of AMP adsorption onto biomimetic apatite, the contribution at 1004 cm^{-1} appears enhanced while the 988 cm^{-1} band does not seem to be present. These observations thus evidence a change in phosphate chemical environments for AMP in the adsorbed state. It therefore indicates that the phosphate group of AMP molecules is also involved in the adsorption process, probably in interaction with calcium ions of the apatite substrate. Note that no obvious band shift was observed on this $\nu_1(PO_4)$ of the apatitic substrate. However, this can probably be explained by the low amount of adsorbed AMP and the relatively low-energy interaction between AMP and apatite as suggested by the ΔG°_{ads} value, "intermediate" between chemisorption and physisorption.

4. Conclusions

The question of how DNA/RNA or their constitutive nucleotides can adsorb on apatitic substrates, independently of the finality (whether related to bone diagenesis or for nanomedicine for example), is an important concern despite the scarce literature on this topic. In this work we investigated the interaction of a model puric-base nucleotide, adenosine monophosphate (AMP), with a biomimetic apatite substrate preliminarily characterized. This study thus complements previous reports relative to the adsorption of double-brand DNA [19] and of a pyrimidic-base nucleotide: cytidine monophosphate (CMP, Choimet et al., publication in progress). Our data indicate that AMP can adsorb onto biomimetic apatite, and the isotherm can be satisfyingly described by the Sips equation, with an exponent greater than unity suggesting some degree of positive cooperativity between adsorbed AMP molecules. The affinity of the surface for AMP was found to be lower than that for CMP, thus evidencing a role of the nature of the nucleic base, which was indeed pointed out via vibrational spectroscopy analyses. This effect would however probably be absent or at least drastically reduced in the case of double-brand DNA where nucleic bases remain in the interior of the double-helix structure, thus becoming inaccessible to direct surface interaction.

The standard Gibbs free energy related to the adsorption process was estimated to about −22 kJ/mol, and this value falls in between the domains often regarded as "physisorption" and "chemisorption". Interestingly, the adsorptive power of biomimetic apatite toward AMP molecules was found to increase significantly in acidic condition (pH 6) as compared to pH 7.4. This effect parallels the one previously observed for DNA adsorption and suggests an apatite surface modification promoting the adsorption of, at least, such phosphate-terminated molecules.

Spectroscopy analyses run before and after adsorption indicated that the global vibrational features of the apatitic substrate essentially remained unchanged upon AMP sorption, but AMP Raman bands (both phosphate and adenine contributions) were found to be significantly modified, pointing to the existence of chemical interactions between AMP molecules and the surface of apatite nanocrystals, and also possibly among adjacent adsorbed species.

This contribution adds to the works being conducted in view of a better understanding of the interaction between biomolecules and the surface of biomimetic apatites, and especially of DNA/RNA and their constitutive nucleotides. It is expected to prove helpful in disciplines such as bone diagenesis sciences or else nanomedicine, among others. Moreover, the question of the start of life on Earth also rises the question of how nucleotides in formation (as future building blocks for DNA) may possibly have been protected against degradation over time: adsorption onto mineral phases such as apatite may have played a non-negligible role in this preservation process. . .

Acknowledgement

The authors thank the University of Sfax for providing financial support to Mr. Khaled Hammami for a doctoral stay in France.

References

[1] J. Gomez-Morales, M. Iafisco, J. Manuel Delgado-Lopez, S. Sarda, C. Drouet, Progress on the preparation of nanocrystalline apatites and surface characterization: overview of fundamental and applied aspects, Progr. Crystal Growth Charact. Mater. 59 (2013) 1–46.

[2] F. Miculescu, G.E. Stan, L.T. Ciocan, M. Miculescu, A. Berbecaru, I. Antoniac, Cortical bone as resource for producing biomimetic materials for clinical use, Digest J. Nanomater. Biostruct. 7 (2012) 1667–1677.

[3] N. Vandecandelaere, C. Rey, C. Drouet, Biomimetic apatite-based biomaterials: on the critical impact of synthesis and post-synthesis parameters, J. Mater. Sci.-Mater. Med. 23 (2012) 2593–2606.

[4] P. Pascaud, P. Gras, Y. Coppel, C. Rey, S. Sarda, Interaction between a bisphosphonate, tiludronate, and biomimetic nanocrystalline apatites, Langmuir 29 (2013) 2224–2232.

[5] B. Palazzo, M. Iafisco, M. Laforgia, N. Margiotta, G. Natile, C.L. Bianchi, et al., Biomimetic hydroxyapatite-drug nanocrystals as potential bone substitutes with antitumor drug delivery properties, Adv. Functional Mater. 17 (2007) 2180–2188.

[6] S. Cazalbou, C. Combes, D. Eichert, C. Rey, M.J. Glimcher, Poorly crystalline apatites: evolution and maturation in vitro and in vivo, J. Bone Miner. Metabol. 22 (2004) 310–317.

[7] D. Eichert, H. Sfihi, C. Combes, C. Rey, Specific characteristics of wet nanocrystalline apatites. Consequences on biomaterials and bone tissue, Bioceramics 16 (2004), 254-2:927-30.
[8] D. Eichert, C. Combes, C. Drouet, C. Rey, Formation and evolution of hydrated surface layers of apatites, Bioceramics 17 (2005) 3–6.
[9] D. Eichert, C. Drouet, H. Sfihi, C. Rey, C. Combes, Nanocrystalline apatite-based biomaterials: synthesis, processing and characterization, in: J.B. Kendall (Ed.), Biomaterials Research Advances, Nova Science Publishers, 2007, pp. 93–143.
[10] C. Rey, J. Lian, M. Grynpas, F. Shapiro, L. Zylberberg, M.J. Glimcher, Non-apatitic environments in bone mineral: FT-IR detection, biological properties and changes in several disease states, Connective Tissue Res. 21 (1989) 267–273.
[11] C. Rey, C. Combes, C. Drouet, H. Sfihi, A. Barroug, Physico-chemical properties of nanocrystalline apatites: implications for biominerals and biomaterials, Mater. Sci. Eng. C 27 (2007) 198–205.
[12] C. Rey, C. Combes., C. Drouet, M. Glimcher, Bone mineral: update on chemical composition and structure, in: 3rd Meeting on Bone Quality, 2009, pp. 1013–1021.
[13] C. Rey, O. Marsan, C. Combes, C. Drouet, D. Grossin, S. Sarda, Characterization of calcium phosphates using vibrational spectroscopies, in: B. Ben-Nissan (Ed.), Advances in Calcium Phosphate Biomaterials, Springer, Berlin Heidelberg, 2014, pp. 229–266.
[14] C. Drouet, M.-T. Carayon, C. Combes, C. Rey, Surface enrichment of biomimetic apatites with biologically-active ions Mg2+ and Sr2+: a preamble to the activation of bone repair materials, Mater. Sci. Eng. C 28 (2008) 1544–1550.
[15] Y. Wu, J.L. Ackerman, E.S. Strawich, C. Rey, H.M. Kim, M.J. Glimcher, Phosphate ions in bone: Identification of a calcium-organic phosphate complex by P-31 solid-state NMR spectroscopy at early stages of mineralization, Calcified Tissue Int. 72 (2003) 610–626.
[16] D. Eichert, C. Drouet, H. Sfihi, C. Rey, C. Combes, Book Chapter: Nanocrystalline apatite based biomaterials: synthesis, processing and characterization. Book: Biomaterials Research Advances, Nova Publisher, 2008, pp. 93–143.
[17] A. Al-Kattan, F. Errassifi, A. Sautereau, S. Sarda, P. Dufour, A. Barroug, et al., Medical potentialities of biomimetic apatites through adsorption, ionic substitution, and mineral/organic associations: three illustrative examples, Adv. Eng. Mater. 12 (2010) B224–B233.
[18] P. Pascaud, F. Errassifi, F. Brouillet, S. Sarda, A. Barroug, A. Legrouri, et al., Adsorption on apatitic calcium phosphates for drug delivery: interaction with bisphosphonate molecules, J. Mater. Sci.-Mater. Med. 25 (2014) 2373–2381.
[19] A. Grunenwald, C. Keyser, A.M. Sautereau, E. Crubezy, B. Ludes, C. Drouet, Adsorption of DNA on biomimetic apatites: toward the understanding of the role of bone and tooth mineral on the preservation of ancient DNA, Appl. Surf. Sci. 292 (2014) 867–875.
[20] A. Grunenwald, C. Keyser, A.M. Sautereau, E. Crubezy, B. Ludes, C. Drouet, Novel contribution on the diagenetic physicochemical features of bone and teeth minerals, as substrates for ancient DNA typing, Anal. Bioanal. Chem. 406 (2014) 4691–4704.
[21] C. Combes, C. Rey, Adsorption of proteins and calcium phosphate materials bioactivity, Biomaterials 23 (2002) 2817–2823.
[22] V. Hlady, J. Buijs, Protein adsorption on solid surfaces, Curr. Opin. Biotechnol. 7 (1996) 72–77.
[23] A.J. Garcia, B.G. Keselowsky, Biomimetic surfaces for control of cell adhesion to facilitate bone formation, Crit. Rev. Eukaryotic Gene Expr. 12 (2002) 151–162.
[24] S. Jebahi, M. Saoudi, R. Badraoui, T. Rebai, H. Oudadesse, Z. Ellouz, et al., Biologic response to carbonated hydroxyapatite associated with orthopedic device: experimental study in a rabbit model, Korean J. Pathol. 46 (2012) 48–54.
[25] P.V. Hauschka, F.H. Wians, Osteocalcin-hydroxyapatite interaction in the extracellular organic matrix of bone, Anatomical Rec. 224 (1989) 180–188.
[26] C. Robinson, S.J. Brookes, J. Kirkham, W.A. Bonass, R.C. Shore, Crystal growth in dental enamel: the role of amelogenins and albumin, Adv. Dental Res. 10 (1996) 173–179, discussion 9-80.
[27] M. Jordan, A. Schallhorn, F.M. Wurm, Transfecting mammalian cells: optimization of critical parameters affecting calcium-phosphate precipitate formation, Nucl. Acids Res. 24 (1996) 596–601.
[28] T. Welzel, I. Radtke, W. Meyer-Zaika, R. Heumann, M. Epple, Transfection of cells with custom-made calcium phosphate nanoparticles coated with DNA, J. Mater. Chem. 14 (2004) 2213–2217.
[29] M. Hermeslima, A.C. Tessis, A. Vieyra, Adsorption of 5'-adenosine monophosphate onto precipitated calcium-phosphate - effects of inorganic polyphosphates and carbamyl-phosphate, Origins Life Evol. Biosphere 20 (1990) 27–41.
[30] S.A. Hawley, J. Boudeau, J.L. Reid, K.J. Mustard, L. Udd, T.P. Makela, et al., Complexes between the LKB1 tumor suppressor, STRAD alpha/beta and MO25 alpha/beta are upstream kinases in the AMP-activated protein kinase cascade, J. Biol. 2 (2003) 28.
[31] T. Forrester, A.R. Lind, Identification of adenosine triphosphate in human plasma and the concentration in the venous effluent of forearm muscles before, during and after sustained contractions, J. Physiol. 204 (1969) 347–364.
[32] B.-K. Son, M. Akishita, K. Iijima, K. Kozaki, K. Maemura, M. Eto, et al., Adiponectin antagonizes stimulatory effect of tumor necrosis factor-alpha on vascular smooth muscle cell calcification: Regulation of growth arrest-specific gene 6-mediated survival pathway by adenosine 5'-monophosphate-activated protein kinase, Endocrinology 149 (2008) 1646–1653.
[33] A. Gee, V.R. Dietz, Determination of phosphate by differential spectrophotometry, Ann. Chem. 25 (1953) 1320–1324.
[34] A.L. Patterson, The Scherrer formula for X-ray particle size determination, Phys. Rev. 56 (1939) 978–982.
[35] A. Boskey, Bone mineral crystal size, Osteoporosis Int. 14 (2003) S16–S20.
[36] S. Cazalbou, G. Bertrand, C. Drouet, Tetracycline-loaded biomimetic apatite: an adsorption study, J. Phys. Chem. B 119 (2015) 3014–3024.
[37] I. Rodriguez-Ruiz, J. Manuel Delgado-Lopez, M.A. Duran-Olivencia, M. Iafisco, A. Tampieri, D. Colangelo, et al., pH-responsive delivery of doxorubicin from citrate-apatite nanocrystals with tailored carbonate content, Langmuir 29 (2013) 8213–8221.
[38] S. Koutsopoulos, Synthesis and characterization of hydroxyapatite crystals: a review study on the analytical methods, J. Biomed. Mater. Res. 62 (2002) 600–612.
[39] C. Drouet, Apatite formation: why it may not work as planned, and how to conclusively identify apatite compounds, Biomed. Res. Int. (2013) 12.
[40] S. Markovic, L. Veselinovic, M.J. Lukic, L. Karanovic, I. Bracko, N. Ignjatovic, et al., Synthetical bone-like and biological hydroxyapatites: a comparative study of crystal structure and morphology, Biomed. Mater. (2011) 6.
[41] H. Elfeki, C. Rey, M. Vignoles, Carbonate ions in apatites - infrared investigations in the NU-4 CO3 domain, Calcified Tissue Int. 49 (1991) 269–274.
[42] H. Elfeki, I. Khattech, M. Jemal, C. Rey, Thermal-decomposition of carbonated hydroxyapatites containing sodium-ions, Thermochim. Acta 237 (1994) 99–110.
[43] A. Grunenwald, C. Keyser, A.M. Sautereau, E. Crubezy, B. Ludes, C. Drouet, Revisiting carbonate quantification in apatite (bio)minerals: a validated FTIR methodology, J. Archaeol. Sci. 49 (2014) 134–141.
[44] E. Koglin, J.M. Sequaris, P. Valenta, Surface Raman-spectra of nucleic-acid components adsorbed at a silver electrode, J. Mol. Struct. 60 (1980) 421–425.
[45] S.A. Lee, A. Anderson, W. Smith, R.H. Griffey, V. Mohan, Temperature-dependent Raman and infrared spectra of nucleosides. Part I—adenosine, J. Raman Spectrosc. 31 (2000) 891–896.
[46] L. Chinsky, P.Y. Turpin, M. Duquesne, J. Brahms, Nucleic-acid derivatives studied by pre-resonance and resonance Raman-spectroscopy in ultraviolet region, Biopolymers 17 (1978) 1347–1359.
[47] L. Rimai, T. Cole, J.L. Parsons, J.T. Hickmott Jr., E.B. Carew, Studies of Raman spectra of water solutions of adenosine tri-, di-, and monophosphate and some related compounds, Biophys. J. 9 (1969) 320–329.